

PAPER • OPEN ACCESS

## Effects of tangential inlet shape and orientation angle on the fluid dynamics characteristics in a biomass burner

To cite this article: Pasyimi *et al* 2018 *J. Phys.: Conf. Ser.* **1090** 012007

View the [article online](#) for updates and enhancements.



**IOP | ebooks™**

Bringing you innovative digital publishing with leading voices to create your essential collection of books in STEM research.

Start exploring the [collection](#) - download the first chapter of every title for free.

# Effects of tangential inlet shape and orientation angle on the fluid dynamics characteristics in a biomass burner

Pasymi<sup>1,2</sup>, Y W Budhi<sup>1</sup> and Y Bindar<sup>1†</sup>

<sup>1</sup> Energy and Processing System Research Group, Study Programmes of Chemical, Bioenergy and Chemurgy Engineerings, Faculty of Industrial Technology, Institut Teknologi Bandung, Indonesia

<sup>2</sup> Department of Chemical Engineering, Faculty of Industrial Technology, Bung Hatta University, Padang, Indonesia

† Corresponding author e-mail: [yazid@che.itb.ac.id](mailto:yazid@che.itb.ac.id)

**Abstract.** The perennial crops are potentially used as renewable fuels in the boiler furnace. Due to its specific characteristics, the burner design for this biomass needs to be properly developed. The burner design proposed here is a cylindrical burner having an axial inlet and a pair of tangential injection. This study is aimed to investigate the effect of tangential inlet geometry on the burner performance, through numerical evaluation of fluid dynamics characteristics. The numerical evaluations are conducted using  $k-\varepsilon$  turbulence model under Ansys-Fluent software. The simulation results showed that, at certain orientation angles of tangential inlet, there are back flows from furnace to the internal burner. This phenomenon is responsible to the flame stability in the burner. The turbulence intensity and convective heat transfer coefficient are also influenced by the tangential inlet orientation angle. For same cross sectional area, the rectangular tangential inlet shape generated deeper backflow penetration and higher turbulence intensity than that was done by the circular ones. One of the rectangular shape shortcomings to the circular ones is to produce the higher static pressure, which correlate to the higher burner operating cost. This investigation study concluded that the burner with rectangular tangential inlet shape and orientation angle of  $20^\circ$  potentially produces the best burner performance.

**Keywords:** backflow penetration, biomass burner, heat transfer coefficient, orientation angle, turbulence intensity, static pressure.

## 1. Introduction

In recent years, along with the depletion of fossil fuel stocks, researchers have begun to develop biomass utilization for electricity generation, particularly for small to medium scale plant [1, 2, 3, 4, 5]. In addition to the renewable objective, biomass is also environmentally friendly ( $\text{CO}_2$  neutral) and has a relatively cheap power generation cost. The perennial crops, one of the non-woody biomass, are proven to be much potential biomass types to be used as fuel in the steam power plant. As an example, *miscanthus x giganteus* has an energy potential of  $\pm 442.5$  GJ/hectare/year and can substitute 20 tons of sub bituminous coal [1].

Generally, burner design is determined by the process occurred in the burner. For solid fuel burners, there are several processes that are expected to take place in a burner, such as the body heating, the devolatilization and the combustion. Some conditions are needed to make processes to take place well in the burner, among others: high temperature, intensive mixing, and sufficient oxygen and residence time [6]. The embodiment of the conditions can be evaluated through the fluid dynamics characteristics in the burner such as turbulence intensity, velocity profile and pressure drop. Furthermore, the velocity profile can illustrate heat transfer rate, residence time and back flow phenomenon.

Some researcher reported that the performance of burner can be increased by involving the tangential flow [7, 8]. The tangential flow has a potential to create the backflow from the furnace to the internal burner. The backflow will carry the hot flue gas from the furnace into the internal burner. This causes the burner temperature to remain high, thus, the process of the particle heating, the devolatilization and



the combustion can take place in the burner, continuously. In addition, the presence of the tangential flow may also increase the mixing intensity. One of the challenges of the tangential flow addition in a burner is to minimize the static pressure. The fluid static pressure is a fluid flow resistant that must be resisted by air blower. The greater the fluid static pressure along the burner, the greater the blower power demand and the greater the burner operational cost becomes.

Currently, the use of the tangential flow in the burner is intensified because of its superiorities. The tangential flow in the burner can be generated through the swirler or through the use of the mechanical devices or through the installation of the tangential injection inlets. The biomass burner proposed here consists of a horizontal cylinder having an internally-extended axial inlet and a pair of tangential injection, as shown in Figure 1.

This research is aimed to study the effects of tangential inlet geometry on the burner performance through the fluid dynamics characteristics evaluation. The tangential inlet geometries studied here are the shape and the orientation angle, while the fluid dynamics characteristics evaluated are turbulence intensity, heat transfer rate, pressure drop and back flow penetration.

The fluid turbulence intensity is represented by the equation (1). Variable  $\bar{u}_i$  is the mean velocity for each direction component and  $u'_i$  is the fluctuation velocity for each direction component [9].

$$I = \frac{\sqrt{((u'_x)^2 + u'_y{}^2 + u'_z{}^2)/3}}{(\bar{u}_x + \bar{u}_y + \bar{u}_z)/3} \quad (1)$$

The heat transfer rate are calculated as convective heat transfer coefficient, as given by equation (2).

$$h = 0.023 \left(\frac{k}{D_c}\right) \left(\frac{\rho D_c \bar{u}}{\mu}\right)^{0.8} \left(\frac{c\mu}{k}\right)^{0.4} \quad (2)$$

Variable  $h$  is convective heat transfer coefficient,  $k$  is thermal conductivity,  $D_c$  is burner diameter,  $c$  is specific heat,  $\rho$  is density and  $\bar{u}$  is magnitude velocity. From equation (2) shown that, for isothermal conditions, the convective heat transfer coefficient is directly proportional to the fluid velocity.

## 2. Investigation methodology

The method used in this research was the Computational Fluid Dynamic (CFD) technique with the Ansys Fluent as the CFD engine. This method has many advantages than experiment, such as low cost, time saving and able to give comprehensive data and information with acceptable results.

### 2.1 Experimental set-up for simulation

The proposed burner design in this study consisted of a horizontal cylindrical body and an inlet section. The inlet section was a certain length cylinder embedded by the internally- extended axial inlet and a pair of tangential injection, as shown in Figure 1. The mixing between the axial and the tangential flows, including their interaction impacts, occurred in the cylindrical body of the burner. The burner fluid dynamics performances were largely determined by the fluid dynamics characteristics in this cylinder. The cylindrical body had a diameter ( $D_c$ ) of 0.3 m and the cylinder aspect ratio ( $L/D_c$ ) of 1.5. The axial inlet was a cylindrical tube with diameter ( $D_{ai}$ ) of 0.15 m.

The tangential inlet has two cross-sectional shape variations those were circular and rectangular shape. The circular shape has a diameter ( $D_{ti}$ ) of 0.062 m, while the rectangular shaped has a width ( $l$ ) of 0.1 m and thickness ( $t$ ) of 0.03 m. The cross-sectional area of the two tangential inlet shape was made equal along the study. The best tangential inlet shape would be chosen to study the effect of orientation angle on the burner fluid dynamics performances. The variations of tangential inlet orientation angle used were  $15^\circ$ ,  $20^\circ$ ,  $25^\circ$ ,  $30^\circ$ ,  $35^\circ$ ,  $40^\circ$ ,  $45^\circ$ ,  $60^\circ$ ,  $75^\circ$  and  $90^\circ$ .

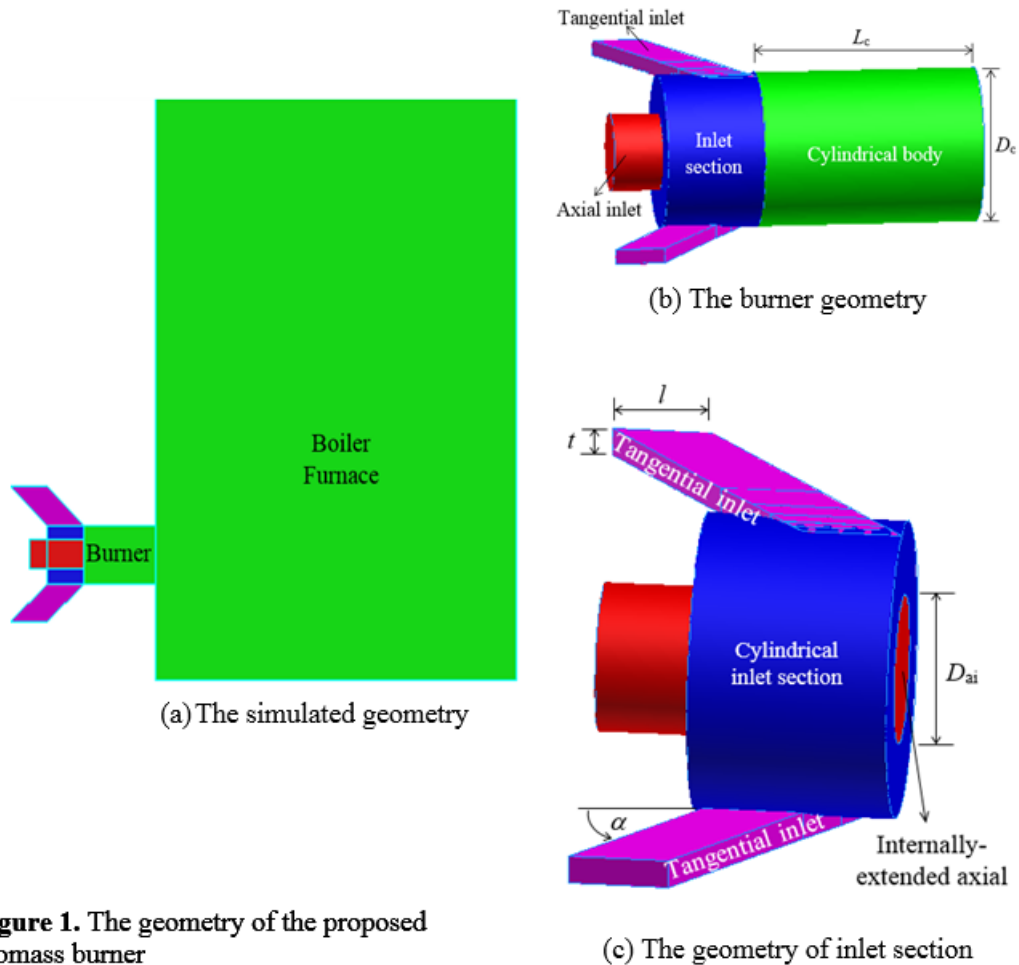


**Figure 1.** The geometry of the proposed biomass burner

The simulation was conducted under the constant burner Reynolds number ( $N_{Re}$ ) and initial tangential intensity ( $I_{it}$ ). All the simulations in this study were conducted on the  $N_{Re}$  of 69,000 and  $I_{it}$  of 3.5. The burner Reynolds number ( $N_{Re}$ ) was calculated using the following formula.

$$N_{Re} = (\rho D_c \bar{u}) / \mu \quad (3)$$

where  $\rho$  is air density,  $D_c$  is burner diameter,  $\bar{u}$  is average magnitude velocity and  $\mu$  is air viscosity.

While, the initial tangential intensity ( $I_{it}$ ) was defined as the ratio of the mass flux entering the tangential inlet to the mass flux of the burner cylinder. Mathematically,  $I_{it}$  could be stated by the following equation

$$I_{it} = (A_c / A_t) \dot{m}_t^2 / (\dot{m}_t + \dot{m}_c)^2 \quad (4)$$

where,  $A_c$  and  $A_t$  are the surface area of burner cylinder and tangential inlet, respectively. Meanwhile  $\dot{m}_t$  and  $\dot{m}_c$  are the mass flowrate entering the tangential inlet and the mass flowrate entering the burner cylinder.

## 2.2 Fluid flow model

Theoretically, fluid dynamics characteristics in a chamber are governed by mass and momentum conservation equations. For constant fluid density ( $\rho$ ) and viscosity ( $\mu$ ), the conservation equations of mass and momentum for turbulent flow were given by the equations (5) to (8). The equations are often known as the Reynolds Average Navier-Stokes (RANS) equations.

$$\frac{\partial \rho}{\partial t} = \frac{\partial \rho \bar{u}_x}{\partial x} + \frac{\partial \rho \bar{u}_y}{\partial y} + \frac{\partial \rho \bar{u}_z}{\partial z} \quad (5)$$

$$\rho \frac{\partial \bar{u}_x}{\partial t} + \sum_{i=x}^{y,z} \rho \bar{u}_i \frac{\partial \bar{u}_x}{\partial i} = -\frac{\partial \bar{p}}{\partial x} + \sum_{i=x}^{y,z} \frac{\partial}{\partial i} \left( \mu_{\text{eff}} \frac{\partial \bar{u}_x}{\partial i} \right) + \rho g_x \quad (6)$$

$$\rho \frac{\partial \bar{u}_y}{\partial t} + \sum_{i=x}^{y,z} \rho \bar{u}_i \frac{\partial \bar{u}_y}{\partial i} = -\frac{\partial \bar{p}}{\partial y} + \sum_{i=x}^{y,z} \frac{\partial}{\partial i} \left( \mu_{\text{eff}} \frac{\partial \bar{u}_y}{\partial i} \right) + \rho g_y \quad (7)$$

$$\rho \frac{\partial \bar{u}_z}{\partial t} + \sum_{i=x}^{y,z} \rho \bar{u}_i \frac{\partial \bar{u}_z}{\partial i} = -\frac{\partial \bar{p}}{\partial z} + \sum_{i=x}^{y,z} \frac{\partial}{\partial i} \left( \mu_{\text{eff}} \frac{\partial \bar{u}_z}{\partial i} \right) + \rho g_z \quad (8)$$

$$\mu_{\text{eff}} = \mu + \mu_t \quad (9)$$

The fluid dynamics equations system above had 5 dependent variables, namely the mean pressure ( $\bar{p}$ ), average velocity of x direction ( $\bar{u}_x$ ), the average velocity of y direction ( $\bar{u}_y$ ), the average velocity of z direction ( $\bar{u}_z$ ) and the turbulent viscosity ( $\mu_t$ ), while the available equations were only 4. There are three methods to solve the above RANS equations system, namely Direct Numerical Solution (DNS) method, modeling method (RANS based model) and Large Eddy Simulation (LES) method. In this research, the solution method used was the modeling with a  $k$ - $\varepsilon$  standard turbulent model. The model was reported by some researchers, has sufficient capability in modeling turbulent swirl flows, especially in low swirl numbers, and has low computational efforts [10, 11].

In the  $k$ - $\varepsilon$  turbulent model, turbulent viscosity ( $\mu_t$ ) is expressed by the equation

$$\mu_t = C_\mu \rho (k^2 / \varepsilon) \quad (10)$$

which  $c_\mu$  is the empirical constant,  $\rho$  is the fluid density,  $k$  is the specific turbulent kinetic energy and  $\varepsilon$  is the dissipation rate of specific turbulent kinetic energy. The occurrence of variables  $k$  and  $\varepsilon$ , resulting in the number of dependent variable on the system of equation is increased to 6 variables, namely ( $\bar{p}$ ), ( $\bar{u}_x$ ), ( $\bar{u}_y$ ), ( $\bar{u}_z$ ),  $k$  and  $\varepsilon$ , while the number of conservation equations available are still 4 equations.

In order to solve simultaneously the above equations system, two additional conservation equations are needed, those are conservation equations for variables  $k$  and  $\varepsilon$ . The formulations of both conservation equations are given by equation (11) and (12).

$$\rho \frac{\partial k}{\partial t} + \sum_{i=x}^{y,z} \rho \bar{u}_i \frac{\partial k}{\partial i} = \sum_{i=x}^{y,z} \frac{\partial}{\partial i} \left( \frac{\mu_{\text{eff}}}{\sigma_k} \frac{\partial k}{\partial i} \right) + G_k - \rho \varepsilon \quad (11)$$

$$\rho \frac{\partial \varepsilon}{\partial t} + \sum_{i=x}^{y,z} \rho \bar{u}_i \frac{\partial \varepsilon}{\partial i} = \sum_{i=x}^{y,z} \frac{\partial}{\partial i} \left( \frac{\mu_{\text{eff}}}{\sigma_\varepsilon} \frac{\partial \varepsilon}{\partial i} \right) + C_{\varepsilon 1} \frac{\varepsilon}{k} G_k - C_{\varepsilon 2} \rho \frac{\varepsilon^2}{k} \quad (12)$$

Thus for  $k$ - $\varepsilon$  turbulent models, fluid dynamics characteristics are simulated by the equations (5) to (8) and equations (11) and (12). Variables  $G_k$  in the above equations is given by the equations (13), while the constant values of each parameter are as follow  $C_\mu = 0.09$ ,  $\sigma_k = 1.0$ ,  $\sigma_\varepsilon = 1.3$ ,  $C_{\varepsilon 1} = 1.44$  and  $C_{\varepsilon 2} = 1.92$  [12].

$$G_k = 2\mu_t \left[ \sum_{i=x}^{y,z} \left( \frac{\partial \bar{u}_i}{\partial i} \right)^2 \right] + \mu_t \left[ \left( \frac{\partial \bar{u}_x}{\partial y} + \frac{\partial \bar{u}_y}{\partial x} \right)^2 + \left( \frac{\partial \bar{u}_x}{\partial z} + \frac{\partial \bar{u}_z}{\partial x} \right)^2 + \left( \frac{\partial \bar{u}_y}{\partial z} + \frac{\partial \bar{u}_z}{\partial y} \right)^2 \right] \quad (13)$$

### 3. Results and discussion

#### 3.1 Effect of tangential inlet cross-sectional shape

The rectangular tangential inlet shape provided a higher turbulence intensity than the circular shape, that was 238.7 versus 208.4%. The predicted heat transfer coefficient generated from the rectangular shape was also larger than the circular ones. The average values of heat transfer coefficient for both of tangential inlet shapes, using the Diffus-Boelter equation, were 32.22 and 29.29 W/m<sup>2</sup>K, respectively. The heat transfer process in the burner has positive correlation to the devolatilization and the combustion process which occurred in the burner.

The rectangular tangential inlet shape resulted in a longer backflow penetration than the circular ones, those were 0.145 and 0.11 m. The comparison of the generated backflow penetration by the two tangential inlet shapes was given in Figure 2. Backflow penetration in this figure was indicated by a negative axial velocity contour. From the picture it was seen that the backflow penetration depth generated by the rectangular tangential inlet shape was longer than the circular shape.

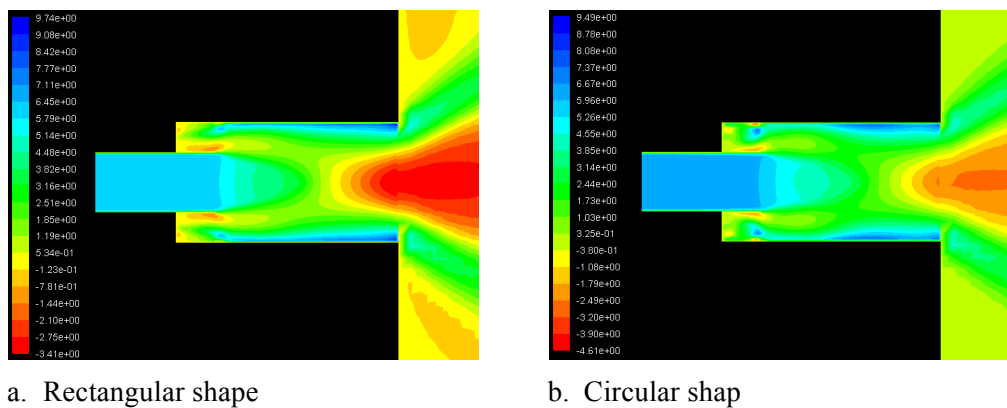


**Figure 2.** Axial velocity contour for both tangential inlet cross section shapes

In the case of the flow resistance, the rectangular tangential inlet shape produced a higher static pressure than the circular ones. The average static pressure in the burner cylinder for both tangential inlet shapes are 51.6 and 42.2 Pascal. The higher the static pressure of the fluid flow, the higher the fluid flow resistance was. It leads to the higher power consumption of the air blower. The comparison of the fluid dynamics performances for both of the tangential inlet shapes were summarized in Table 1.

**Table 1.** Comparison of fluid dynamics performances of rectangular and circular tangential inlet shapes.

Performance parameter	Tangential inlet shape	
	Circular	Recta
Turbulence intensity, %	208.4	238.7
Heat transfer coef., W/m <sup>2</sup> K	29.29	32.22
Backflow penetration, m	0.11	0.145
Static pressure, Pascal	42.2	51.6

#### 3.2 Effect of tangential inlet orientation angle

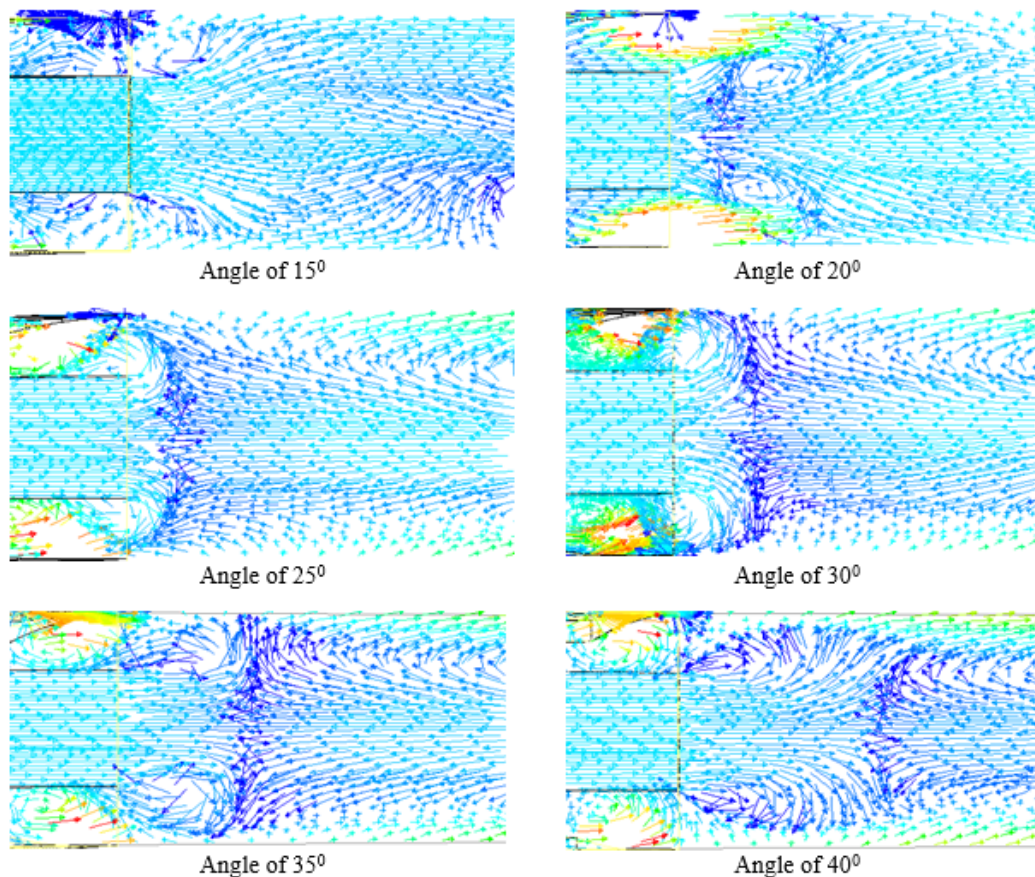
The tangential inlet angle also affects the fluid dynamics characteristics in the burner cylinder. When the orientation of tangential inlet configures a certain angle with the axial axis, then the stream that is formed from the inlet will be tangentially oriented. The larger the tangential inlet angle, the greater the tangential flow frequency and vice versa.

Research on the influence of tangential inlet orientation angle to the burner performance was reported by Ziqiang et al (2016). Of the 3 tangential inlet orientation angles used, ie, 15<sup>0</sup>, 30<sup>0</sup> and 45<sup>0</sup>, Ziqiang stated that the best tangential inlet orientation angle is an angle of 30<sup>0</sup>. At that angle, the largest recirculation zones and uniformly dispersed fuels in the furnace were produced [13].

To see the effect of the other orientation angle in the range of  $15^{\circ}$  to  $45^{\circ}$ , the tangential inlet angle was varied every  $5^{\circ}$ . In addition, the orientation angles greater than  $45^{\circ}$ , namely  $60^{\circ}$ ,  $75^{\circ}$  and  $90^{\circ}$ , were also simulated. Besides being evaluated based on the recirculation flow pattern, the burner fluid dynamics performances were also evaluated based on other variables such as turbulence intensity, heat transfer and static pressure.

From all tangential inlet orientation angles simulated, the backflow from the furnace to the internal burner always exists, except for the orientation angle of  $15^{\circ}$ . The tendency of penetration depth could be stated as the greater the orientation angle, the shorter the backflow penetration depth and vice versa. There is no backflow from the furnace to the internal burner, at the orientation angle of  $15^{\circ}$ , is due to the low frequency of the tangential flow that is formed at this angle.

At the orientation angle of  $20^{\circ}$ , the backflow penetration approaches the axial inlet output. The mixture of the incoming flow and backflow recirculate to the furnace through the area near the wall. At orientation angles of  $25^{\circ}$  and  $30^{\circ}$ , although the depth of backflow penetration is close to the axial inlet output, but the mixture of the two streams tends to lead to the tangential inlet section. For the larger orientation angles ( $35^{\circ}$ ,  $40^{\circ}$ ,  $45^{\circ}$ ,  $60^{\circ}$ ,  $75^{\circ}$  and  $90^{\circ}$ ), the depth of backflow penetration is shorter. A comparison of the backflow pattern in the burner cylinder for some tangential inlet orientation angles is given in the figure 3.



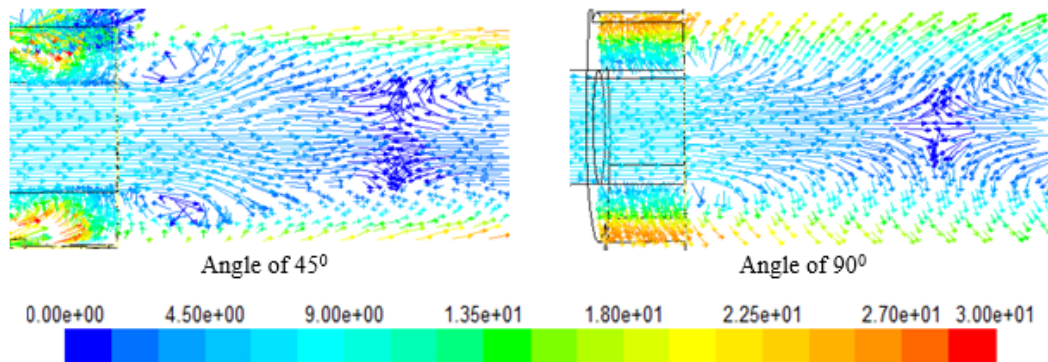


**Figure 3.** Recirculation flow pattern in burner cylinder for various tangential inlet orientation angles

In term of mixing intensity, the tangential inlet with orientation angle  $20^\circ$  yielded the highest turbulence intensity value. This condition is related to the formation of internal recirculation at the mixing zone of the two flow streams. In addition, on this orientation angle, the static pressure was relatively low and the heat transfer rate was relatively high, as shown in figure 4. This indicates that the burner with the tangential inlet angle of  $20^\circ$  has the potential to produce the best fluid dynamics performance in the burner. It will allow the devolatilization process and a stable ignition occurs in the burner.

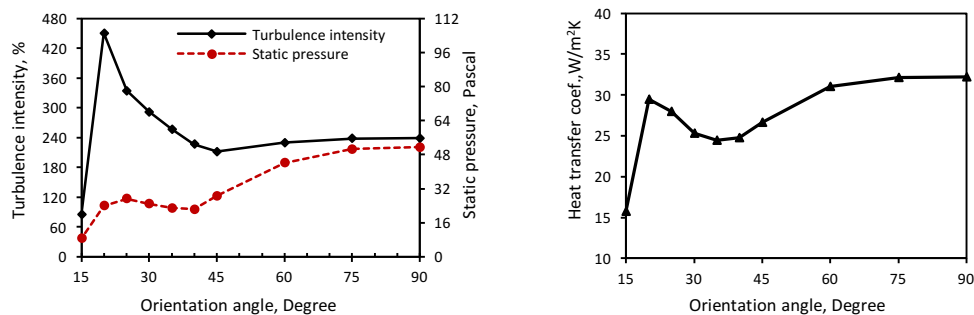


**Figure 4.** Profile of turbulence intensity, static pressure and heat transfer coefficient in burner cylinder for several tangential inlet orientation angles.

#### 4. Conclusion

The fluid dynamics characteristics in the proposed biomass burner design have been simulated using a standard  $k-\varepsilon$  turbulent model. The simulation results showed that orientation angle and shape of the tangential inlet influence significantly the fluid dynamic characteristics in the burner cylinder.

At certain orientation angle, the tangential inlet tends to produce back flow from furnace to the internal burner. The tendency of back flow penetration depth could be stated as the greater the orientation angle, the shorter the backflow penetration depth. The turbulence intensity is also inversely proportional to the tangential inlet orientation angle, while the static pressure and heat transfer coefficient are directly proportional to it. The rectangular tangential inlet shape produces the deeper backflow penetration depth, the higher turbulence intensity and the greater heat transfer rate, but it requires a higher blower power than the circular shape to overcome the greater static pressure.

The above results have revealed that the best tangential inlet orientation angle of the proposed biomass burner is  $20^\circ$  and the appropriate tangential inlet shape is rectangular. Under these conditions, the fluid dynamics characteristics in the burner cylinder potentially produce the best burner performance.



### Acknowledgments

We would like to thank to the Ministry of Research, Technology and Higher Education of Indonesia for the awarded research fund to this research on the decentralization research scheme.

### References

- [1] Dahl J dan Obernberger I 2004 *2nd World Conference on Biomass for Energy, Industry and Climate Protection* Rome Italy
- [2] Kops S M B and Malte P C 2004 *Final Technical Report, Energy and Environmental Combustion Laboratory* Department of Mechanical Engineering University of Washington
- [3] Siyi L, Bo X, Zhiquan H, Liu S and Maoyun H 2010 *Energy Conversion and Management* **51** 2098-2102
- [4] Momeni M, Yin C, Kær S K, Hansen T B, Jensen P A and Glarborg P 2013 *Energy & Fuels* **27** 507–14
- [5] Arnao J H S, Ferreira D J O, Santos C G, Alvarez J E, Rangel L P and Park S W 2015 *International Journal of Mechanical, Aerospace, Industrial, Mechatronic and Manufacturing Engineering* **9** (5) 798-801
- [6] Nag P K 2002 *Power Plant Engineering* 2<sup>nd</sup> edition (Singapore: McGraw Hill Company)
- [7] Paulrud S dan Nilsson C 2004 *Fuel* **83** 813-21
- [8] Al-Abdeli Y M and Masri A R 2015 *Experimental Thermal and Fluid Science* (Accepted Manuscript)
- [9] Ansys Incorporation. 2013 *Solver Theory* (United States: Canonsburg)
- [10] Nemoda S, Bakic V, Oka S, Zivkovic G and Crnomarkavic N 2005 *Int. J. Heat Mass Transfer* **48** 4623–32
- [11] Vazquez J A R 2012 *Thesis* University of Zaragoza Spain
- [12] Yazid B 2017 *Rekayasa Komputasi Aliran Turbulen Multidimensi* First edition (Bandung: ITB Press) pp 18-24
- [13] Ziqiang L V, Guangqiang L and Yingjie L 2016 *International Journal of Smart Home* **10** 171-80